Fast spike train inference from calcium imaging

Joshua T. Vogelstein, others, Liam Paninski

May 26, 2009

Abstract

Experiments often yield measurements of variables that are naturally constrained to be nonnegative. In such scenarios, it may be desirable to filter (or deconvolve) the observations to find the most likely trajectory of the nonnegative variable, given the noisy observations. Here, we develop a computationally-efficient optimal filter for a certain subset of nonnegatively constrained deconvolutions. Specifically, for any nonnegative variable that is filtered by a matrix linear differential equation and observed with independent, log-concave noise, we can infer the optimal nonnegative trajectory via straightforward interior-point methods in $O(T)$ (linear) time, as opposed to more standard approaches requiring $O(T^3)$ time (where T is the total number of time steps). The key is to make use of the tridiagonal structure of the Hessian of the log-posterior here, which allows us to perform each Newton iteration in linear time. We apply this filter to an important problem in neuroscience: inferring a spike train from noisy calcium fluorescence observations. We demonstrate the filter's improved performance on simulated and real data. In conclusion, we propose that this filter is readily applicable for a number of real-time applications, including spike inference from simultaneously-observed large neural populations.

1 Introduction

2 Methods

2.1 Model

We assume a simple discrete-time state-space model relating spikes, n_t, baseline subtracted intracellular calcium concentration, denoted by C_t, and fluorescence measurements, F_t. First, we assume a linear relationship between F_t and C_t, with gaussian noise. Second, we assume that C_t jumps after each spike, and then decays according to some time constant. Finally, we assume that spikes are distributed according to a Poisson process. The above assumptions lead to the follwoing model:

$$\boldsymbol{F}_t = \boldsymbol{\alpha}(C_t + \beta) + \boldsymbol{\varepsilon}_t, \qquad \boldsymbol{\varepsilon}_t \sim \mathcal{N}(\boldsymbol{0}, \sigma^2 \boldsymbol{I}) \tag{1}$$

$$C_t = \gamma C_{t-1} + n_t, \qquad n_t \sim \text{Poisson}(n_t; \lambda\Delta) \tag{2}$$

where $\boldsymbol{\alpha}$ and β set the fluorescence spatial filter and offset respectively, σ^2 indicates the variance of the noise, and γ sets the decay rate.

2.2 Inference

Given such a model, our goal is to find the maximum *a posteriori* (MAP) spike train, i.e., the most likely spike train, $\boldsymbol{n}$ (where we use the shorthand notation $\boldsymbol{X} = [X_1, \ldots, X_T]$, and T is the final time step), given the fluorescence measurements, $\boldsymbol{F}$. Thus, the objective function that we'd like to solve may be written as:

$$\widehat{\boldsymbol{n}} = \operatorname*{argmin}_{n_t \in \mathbb{N}_0 \forall t} P[\boldsymbol{n}|\boldsymbol{F}] = \operatorname*{argmin}_{n_t \in \mathbb{N}_0 \forall t} P[\boldsymbol{F}|\boldsymbol{n}]P[\boldsymbol{n}]$$

$$= \operatorname*{argmax}_{n_t \in \mathbb{N}_0 \forall t} \prod_{t=1}^{T} P[\boldsymbol{F}_t|C_t]P[n_t] = \operatorname*{argmax}_{n_t \in \mathbb{N}_0 \forall t} \sum_{t=1}^{T} \left(\log P[\boldsymbol{F}_t|C_t] + \log P[n_t] \right)$$

$$= \operatorname*{argmin}_{n_t \in \mathbb{N}_0 \forall t} \sum_{t=1}^{T} \left(\frac{1}{2\sigma^2} \|\boldsymbol{F}_t - \boldsymbol{\alpha}(C_t + \beta)\|^2 - n_t \log \lambda\Delta + \log n_t! \right), \tag{3}$$

where $\mathbb{N}_0 = \{0, 1, 2, \ldots\}$, and C_t is implicitly a function of n_t. Unfortunately, the computational complexity of solving Eq. (3) scales exponentially with T, i.e., is $O(\mathrm{e}^T)$, making Eq. (3) an NP-hard problem. Thus, instead of an exact solution, we propose to make an approximation that reduces the complexity to be *polynomial* in T. In particular, we relax the assumption that we must have an integer number of spikes at any time step, by approximating the Poisson distribution with an exponential. Note that this is a common approximation technique in the machine learning literature [Hastie et al., 2001], as it is the closest convex relaxation to its non-convex counterpart. The constraint on n_t in Eq. (3) is therefore relaxed from $n_t \in \mathbb{N}_0$ to $n_t \geq 0$:

$$\widehat{\boldsymbol{n}} \approx \operatorname*{argmin}_{n_t \geq 0 \forall t} \sum_{t=1}^{T} \left(\frac{1}{2\sigma^2} (\|\boldsymbol{F}_t - \boldsymbol{\alpha}(C_t + \beta)\|^2 + n_t \lambda\Delta) \right). \tag{4}$$

While this convex relaxation makes the problem tractable, the "sharp" threshold imposed by the nonnegativity constraint prohibits the use of standard gradient ascent techniques [Boyd and Vandenberghe, 2004]. We therefore take an "interior-point" (or "barrier") approach, in which we drop the sharp threshold, and add a barrier term, which must approach $-\infty$ as n_t approaches zero (e.g., $-\log n_t$) [Boyd and Vandenberghe, 2004]. By iteratively reducing the weight of the barrier term, $z > 0$, we are guaranteed to converge to the correct solution [Boyd and Vandenberghe, 2004], $\widehat{\boldsymbol{n}}$. Thus, our goal is to efficiently solve:

$$\widehat{\boldsymbol{n}}_z = \operatorname*{argmin}_{n_t \forall t} \sum_{t=1}^{T} \left(\frac{1}{2\sigma^2} \|\boldsymbol{F}_t - \boldsymbol{\alpha}(C_t + \beta)\|^2 + n_t \lambda\Delta - z \log(n_t) \right), \tag{5}$$

which is concave and may therefore be solved exactly and efficiently using a gradient ascent technique. To see how, we first note that spikes and calcium are related to one another via a simple linear transformation, namely, $n_t = f(C_t, C_{t-1}) = C_t - \gamma C_{t-1}$, or, in matrix notation:

$$\boldsymbol{MC} = \begin{bmatrix} 1 & 0 & 0 & \cdots & \cdots \\ 1 & -\gamma & 0 & \cdots & \cdots \\ 0 & 1 & -\gamma & 0 & \cdots \\ \vdots & \vdots & \vdots & \vdots & \vdots \\ 0 & 0 & 0 & 1 & -\gamma \end{bmatrix} \begin{bmatrix} C_1 \\ C_2 \\ \vdots \\ \vdots \\ C_T \end{bmatrix} = \begin{bmatrix} n_1 \\ n_2 \\ \vdots \\ \vdots \\ n_T \end{bmatrix} = \boldsymbol{n} \tag{6}$$

where $\boldsymbol{M} \in \mathbb{R}^{T \times T}$ is a bidiagonal matrix, and $\boldsymbol{C} = (C_1, \ldots, C_T)^\mathsf{T}$ and $\boldsymbol{n}$ are T dimensional column vectors ($^\mathsf{T}$ indicates matrix transpose). Given Eq. (6), we may rewrite Eq. (5) in terms of $\boldsymbol{C}$:

$$\widehat{\boldsymbol{C}}_z = \operatorname*{argmin}_{C_t - \gamma C_{t-1} \geq 0 \forall t} \sum_{t=1}^{T} \left(\frac{1}{2\sigma^2} \|\boldsymbol{F}_t - \boldsymbol{\alpha}(C_t + \beta)\|^2 + (C_t - \gamma C_{t-1})\lambda\Delta - z \log(C_t - \gamma C_{-1} - \nu) \right)$$

$$= \operatorname*{argmin}_{\boldsymbol{MC} \geq \boldsymbol{0}} \frac{1}{2\sigma^2} \left\| \boldsymbol{F} - \boldsymbol{\alpha}(\boldsymbol{C}^\mathsf{T} + \beta) \right\|^2 + \lambda\Delta(\boldsymbol{MC})^\mathsf{T}\boldsymbol{1} - z \log(\boldsymbol{MC})^\mathsf{T}\boldsymbol{1}, \tag{7}$$

where $\boldsymbol{MC} \geq \boldsymbol{0}$ indicates that every element of $\boldsymbol{MC}$ is greater than or equal to zero, $'$ indicates transpose, and $\boldsymbol{1}$ is a T dimensional column vector, and $\log(\cdot)$ indicates an element-wise logarithm. As (7) is concave (it is identical to Eq. (5) with different notation), we may use any descent technique to find $\widehat{\boldsymbol{C}}_z$. We elect to use the Newton-Raphson approach:

$$\widehat{\boldsymbol{C}}_z \leftarrow \widehat{\boldsymbol{C}}_z + s\boldsymbol{d} \tag{8a}$$

$$\boldsymbol{H}\boldsymbol{d} = \boldsymbol{g} \tag{8b}$$

$$\boldsymbol{g} = -\frac{\boldsymbol{\alpha}}{\sigma^2}(\boldsymbol{F} - \boldsymbol{\alpha}(\widehat{\boldsymbol{C}}_z^\mathsf{T} + \beta)) + \lambda\Delta\boldsymbol{M}^\mathsf{T}\boldsymbol{1} - z\boldsymbol{M}^\mathsf{T}(\boldsymbol{M}\widehat{\boldsymbol{C}}_z)^{-1} \tag{8c}$$

$$\boldsymbol{H} = \frac{\boldsymbol{\alpha}^2}{\sigma^2}\boldsymbol{I} + z\boldsymbol{M}^\mathsf{T}(\boldsymbol{M}\widehat{\boldsymbol{C}}_z)^{-2}\boldsymbol{M} \tag{8d}$$

where s is the step size, $\boldsymbol{d}$ is the step direction, and $\boldsymbol{g}$ and $\boldsymbol{H}$ are the gradient (first derivative) and Hessian (second derivative) of the likelihood, respectively (the likelihood is the argument to be minimized in Eq. (7)), and the exponents indicate element-wise operations. Note that we use "backtracking linesearches", meaning that for each iteration, we find the maximal s that is between 0 and 1 and decreases the likelihood.

Typically, implementing Newton-Raphson requires inverting the Hessian, i.e., $\boldsymbol{d} = \boldsymbol{H}^{-1}\boldsymbol{g}$, a computation consuming $O(T^3)$ time. Instead, because $\boldsymbol{M}$ is bidiagonal, the Hessian is tridiagonal, so the solution may be found in $O(T)$ time via standard banded Gaussian elimination techniques (which can be implemented efficiently in Matlab using $\boldsymbol{H} \backslash \boldsymbol{g}$). The resulting fast algorithm for solving the optimization problem in (4) is the main result of this paper, i.e. we may approximately infer the optimal solution for models characterized by equations such as (1) and (2) in linear time, whereas an exact solution would require exponential time, and a naïve approximate solution would require polynomial time.

2.3   Learning

In the above, we assumed that the parameters governing our model, $\boldsymbol{\theta} = \{\boldsymbol{\alpha}, \beta, \sigma, \gamma, \nu, \rho.\lambda\} \in \boldsymbol{\Theta}$, were known. In general, however, these parameters may be estimated from the data. To find the maximum likelihood estimator for the parameters, $\widehat{\boldsymbol{\theta}}$, we must integrate over the unknown variable, $\boldsymbol{n}$. However, integrating over all possible spike trains is typically approximated by Monte Carlo approaches, which is relatively slow. Thus, one often approximates:

$$\widehat{\boldsymbol{\theta}} = \operatorname*{argmax}_{\boldsymbol{\theta} \in \boldsymbol{\Theta}} \iint P[\boldsymbol{F}|\boldsymbol{C}, \boldsymbol{n}, \boldsymbol{\theta}]P[\boldsymbol{C}, \boldsymbol{n}|\boldsymbol{\theta}]d\boldsymbol{n}d\boldsymbol{C} \approx \operatorname*{argmax}_{\boldsymbol{\theta} \in \boldsymbol{\Theta}} P[\boldsymbol{F}|\widehat{\boldsymbol{C}}, \widehat{\boldsymbol{n}}, \boldsymbol{\theta}]P[\widehat{\boldsymbol{C}}, \widehat{\boldsymbol{n}}|\boldsymbol{\theta}] \tag{9}$$

where $\widehat{\boldsymbol{n}} = [\widehat{n}_1, \ldots, \widehat{n}_T]$ is estimate of $\widehat{\boldsymbol{n}}$ from the inference algorithm described above ($\widehat{\boldsymbol{C}}$ is defined similarly). The approximation in (14) is good whenever the likelihood is very peaky, meaning that most of the mass is around the MAP sequence.[1] In particular, for state-space models, one often approximates the integral in (14) with the Viterbi path, i.e., the MAP path of the hidden states [Rabiner, 1989]. Finding the Viterbi path is often far easier than solving the integral in (14), as in the case here. Due to the state space nature of the above model (Eqs (1) and (2)), the optimization in Eq (9) simplifies significantly. More specifically, we can write the argument from the left-hand-side of Eq (9) as a product of terms that we have defined in our model:

$$P[\boldsymbol{F}|\widehat{\boldsymbol{C}}, \widehat{\boldsymbol{n}}, \boldsymbol{\theta}]P[\widehat{\boldsymbol{C}}, \widehat{\boldsymbol{n}}|\boldsymbol{\theta}] = \prod_{t=1}^{T} P[F_t|\widehat{C}_t, \boldsymbol{\alpha}, \beta, \sigma]P[\widehat{C}_t|\widehat{C}_{t-1}, \widehat{n}_t, \gamma]P[\widehat{n}_t|\lambda] \tag{10}$$

Thus, this likelihood is jointly concave in all the parameters. To solve for $\{\boldsymbol{\alpha}, \beta, \sigma\}$, we solve:

---

[1] The approximation in (14) may be considered a first-order Laplace approximation

$$\{\widehat{\alpha}, \widehat{\beta}, \widehat{\sigma}\} = \underset{\boldsymbol{\alpha}, \beta, \sigma > 0}{\operatorname{argmax}} \sum_{t=1}^{T} \log P[F_t | \widehat{C}_t, \boldsymbol{\alpha}, \beta, \sigma]$$

$$= \underset{\boldsymbol{\alpha}, \beta, \sigma > 0}{\operatorname{argmax}} -\frac{T}{2} \log(2\pi\sigma^2) - \frac{1}{2\sigma^2} \sum_{t=1}^{T} (F_t - \boldsymbol{\alpha}\widehat{C}_t - \beta)^2$$

$$= \underset{\boldsymbol{\alpha}, \beta, \sigma > 0}{\operatorname{argmax}} -\frac{T}{2} \log(2\pi\sigma^2) - \frac{1}{2\sigma^2} \left\| \boldsymbol{F} - \widehat{\boldsymbol{X}}\boldsymbol{\eta} \right\|^2 \qquad (11)$$

where $\boldsymbol{\eta} = [\boldsymbol{\alpha}, \beta]$ and $\widehat{\boldsymbol{X}}_t = [\widehat{C}_t, 1]$. Thus, solving for $\{\widehat{\alpha}, \widehat{\beta}\}$, is a constrained quadratic optimization problem, which can be solved efficiently using standard tools, such as Matlab's `quadprog`. The variance may then be solved for analytically:

$$\widehat{\sigma}^2 = \frac{1}{T} \left\| \boldsymbol{F} - \widehat{\boldsymbol{X}}\widehat{\boldsymbol{\eta}} \right\|_2^2 \qquad (12)$$

Similarly, taking the log of the prior term, $P[\widehat{\boldsymbol{n}}|\boldsymbol{\theta}]$ yields:

$$\log P[\widehat{\boldsymbol{n}}|\boldsymbol{\theta}] = \sum_{t=1}^{T} \log(\lambda\Delta) - \lambda\Delta\widehat{n}_t = T(\lambda\Delta) - \lambda\Delta\widehat{\boldsymbol{n}}'\boldsymbol{1} \qquad (13)$$

Plugging Eqs (11) and (13) back into Eq (9), and noting that log is a monotonic function, we have:

$$\widehat{\boldsymbol{\theta}} = \underset{\boldsymbol{\theta} \in \boldsymbol{\Theta}}{\operatorname{argmax}} -\frac{T}{2} \log(2\pi\sigma^2) - \frac{1}{2\sigma^2} \left\| \boldsymbol{F} - \widehat{\boldsymbol{X}}\boldsymbol{\eta} \right\|_2^2 + T\log(\lambda\Delta) - \lambda\Delta\widehat{\boldsymbol{n}}'\boldsymbol{1} \qquad (14)$$

Estimating the parameters then separates into three log-concave problems. In particular, solving for $\widehat{\boldsymbol{\eta}}$ is simply:

$$\widehat{\boldsymbol{\eta}} = \underset{\boldsymbol{\eta}, \, 0 < \eta_1 < 1}{\operatorname{argmin}} \frac{1}{2} \left\| \boldsymbol{F} - \widehat{\boldsymbol{X}}\boldsymbol{\eta} \right\|_2^2 = \underset{\boldsymbol{\eta}, \, 0 < \eta_1 < 1}{\operatorname{argmin}} \frac{1}{2} \boldsymbol{\eta}'\boldsymbol{Q}\boldsymbol{\eta} - \boldsymbol{L}'\boldsymbol{\eta} \qquad (15)$$

where $\boldsymbol{Q} = \widehat{\boldsymbol{X}}'\widehat{\boldsymbol{X}}$, and $\boldsymbol{L} = \widehat{\boldsymbol{X}}'\boldsymbol{F}$, and the constraint, $0 < \eta_1 < 1$, ensures that the time constant is both non-negative and finite. Eq (15) may be solved using standard quadratic optimization tools, such as Matlab's `quadprog`.

Unfortunately, the recursive nature of our algorithm makes solving for $\widehat{\boldsymbol{\eta}}$ in this manner unidentifiable. In particular, because both $\widehat{\boldsymbol{X}}$ and $\boldsymbol{\eta}$ can scale and shift $\boldsymbol{C}$, alternating between inferring $\widehat{\boldsymbol{X}}$ and $\widehat{\boldsymbol{\eta}}$ does not converge (data not shown). However, this is not particularly problematic, because the fluorescence measurements are in arbitrary units. This unit arbitrariness suggests that $\boldsymbol{F}$ may be scaled and shift without loss of generality. The prior term and non-negativity constraint on $\boldsymbol{n}$, however, imposes small costs associated with scaling and shifting $\boldsymbol{n}$ and $\boldsymbol{C}$. We therefore estimate $\boldsymbol{\eta}$ from the raw fluorescence trace. More specifically, to estimate γ, we manually find a fluorescence sequence that seem to be decaying, estimate the time constant τ, and let $\gamma = 1 - \Delta/\tau$. For ν, we manually find a fluorescence sequence that seems to be near baseline, label it $[F_s, \dots, F_t]$, and let $\nu = \frac{1}{t-s} \sum_{u=s}^{t} F_u$. Finally, we estimate ρ by letting it be equal to what we manually determine it be, by eye. In practice, we have found that by first scaling and shifting $\boldsymbol{F}$ to be between 0 and 1, subsequent traces from the same or different cells have very similar values for $\boldsymbol{\eta}$, and therefore, these parameters need not be tweaked much. Furthermore, the effective signal-to-noise ratio (SNR) of the inferred spike train does not depend strongly on these parameters, in agreement with previous results [Yaksi and Friedrich, 2006]. The other parameters, σ and λ, can be solved for analytically:

$$\widehat{\sigma}^2 = \frac{1}{T} \left\| \boldsymbol{F} - \widehat{\boldsymbol{X}}\widehat{\boldsymbol{\eta}} \right\|_2^2 \qquad (16)$$

$$\widehat{\lambda} = \frac{1}{T\Delta} \widehat{\boldsymbol{n}}'\boldsymbol{1} \qquad (17)$$

3 Results

3.1   Main Result

To evaluate the efficacy of our fast filter, we compare it with the optimal linear (i.e., Wiener) filter [Wiener, 1949]. The top three panels of Fig. 1 depict a typical dataset simulated according to our model, Eqs. (1) and (2). Beneath the simulation, we show both the Wiener filter output (fourth panel) and our fast filter output (bottom panel). For both filters, we provided only the fluorescence observations depicted in the top panel, and η. From this data, we estimate the remaining parameters, and infer the hidden spike train. Several differences between these two approaches should be apparent. First, the effective signal-to-noise ratio (SNR) of our fast filter improves upon the optimal linear filter. Second, while the Wiener filter induces a "ringing" effect (where the inferred signal oscillates above and below zero), our fast filter completely eliminates this effect. These two improvements are common observations upon imposing a non-negative constraint when appropriate [Shumway and Stoffer, 2006]. Importantly, both our implementation of the Wiener filter and our fast filter require only $O(T)$ time, whereas the naïve implementation of the Wiener filter requires $O(T \log(T))$, and the naïve implementation of a non-negative filter requires $O(T^3)$. Thus, when our approximation in Eq (4) is good, our filter outperforms the Wiener filter, and imposes approximately the same computational burden.
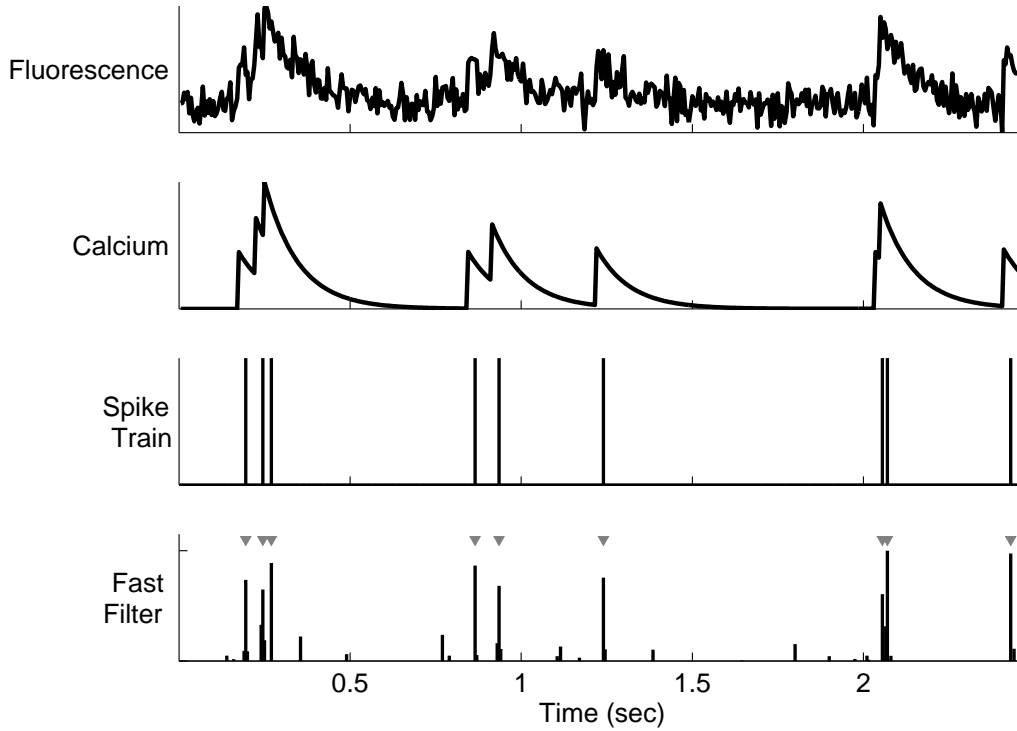

Figure 1: A simulation demonstrating that given a fluorescence time series, and the parameters of our model, we can accurately infer a close approximation to the most likely spike train. Top panel: simulated fluorescence time series. Second panel: simulated intracellular calcium concentration. Third panel: simulated spike train. Fourth panel: the fast filter's inferred spike train (gray triangles indicate true spike times here, and elsewhere, unless indicated otherwise). Parameters: $\Delta = 5$ msec, $\alpha = 1$ photons/μM., $\beta = 0$ unitless, $\sigma = 0.25$ photons, $\tau = 100$ msec, $\lambda = 5$ Hz.

3.2   Comparison with Wiener filter

When the observed neuron is spiking quickly, the Poisson distribution may be well approximated by a Gaussian distribution, suggesting that the Wiener filter may be optimal in this regime. But the exponential approximation of a Poisson is also very accurate in the fast spiking regime. To compare these two strategies, we simulated a fast spiking neuron, where the expected number of spikes per bin exceeds 10 (Fig. **??**). In this scenario, both the Wiener filter and our fast filter perform approximately equally well. Both filters infer peaks in the firing rate that are obscured by the low-pass filter properties of the calcium dynamics. Thus, it seems from this analysis that regardless of the firing rate of the observable neuron, (1) filtering the signal may provide valuable information, and (2) our fast filter performs at least as well as the Wiener filter, without requiring more computational time.
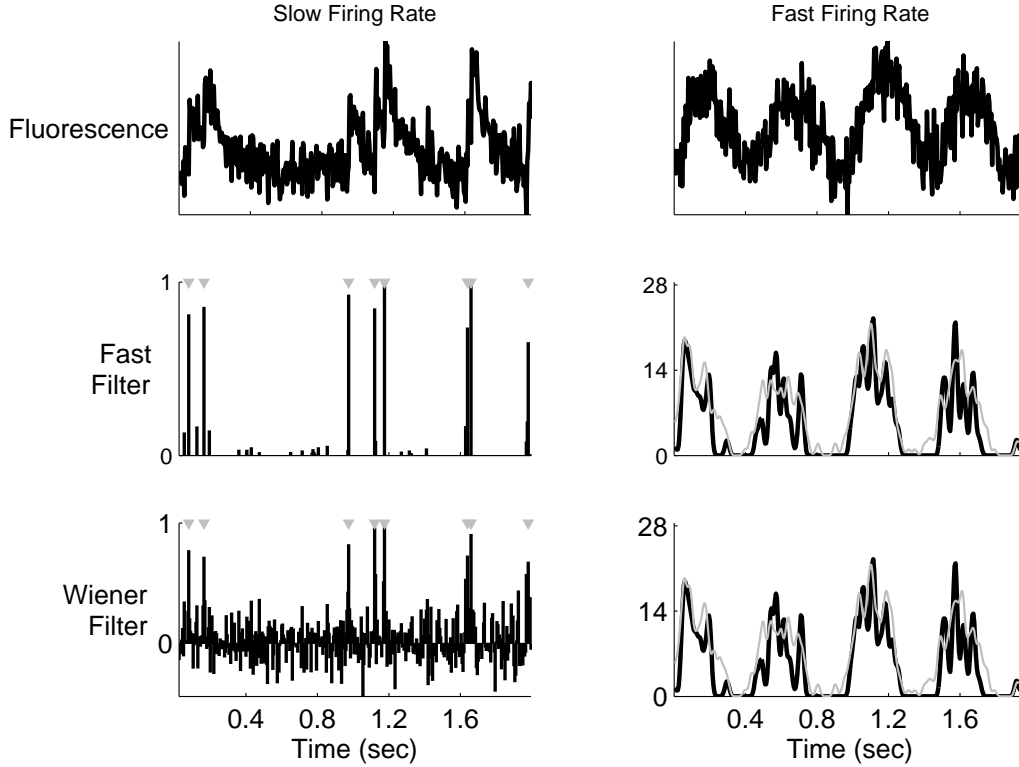

Figure 2: A simulation demonstrating that the fast filter performs at least as well as the optimal linear filter. The left panels show that in the slow firing regime, the fast filter — which approximates the Poisson distribution governing spiking with an exponential distribution — outperforms the Wiener filter — which approximates the Poisson distribution with a Gaussian. The right panels show that both approximations are sufficient in the fast firing regime. Top left panel: fluorescence time series for a neuron with a slow firing rate. Middle left panel: the fast filter's inferred spike train. Bottom left panel: Wiener filter's inferred spike train. Note that (i) the Wiener filter does not impose a non-negativity constraint, and (ii) the effective SNR of this filter in this example is higher than the fast filter's. Top right panel: same as top left panel, for a neuron with a high firing rate. Middle right panel: the fast filter's inferred spike train smoothed with a Gaussian kernel for visualization purposes (black line), and the true spike train smoothed with the same Gaussian kernel (gray line). Bottom right panel: same as middle right panel, but with the Wiener filter. Parameters for left panels: same as above. Parameters for right panels: same as above, except: $\sigma = 8$ photons, $\lambda = 500$ Hz.

3.3   Spatial Filtering

In the above, we assumed a one-dimensional (1-D) observation, $\boldsymbol{F}$. The raw data, however, is actually a series of multidimensional images. To get the 1-D time-series, two pre-processing steps are required. First, for each neuron, one must define a region-of-interest (ROI), essentially assigning sets of pixels to neurons. This yields a vector time-series for each neuron, $\vec{\boldsymbol{F}}_t \in \mathbb{R}^m$. Second, one must project the $m-$D observations into a 1-D time-series. Typically, this step is performed by averaging all the pixels within the ROI. In theory, one can improve on this uniform averaging by estimating the optimal spatial filter. Here, we provide details on how to incorporate this second step (projecting the $m-$D observations into 1-D) into our fast filter. First, we replace Eq (3) with:

$$\vec{\boldsymbol{F}}_t = \boldsymbol{\alpha} C_t + \boldsymbol{\beta} + \boldsymbol{\Sigma}\boldsymbol{\varepsilon}_t, \qquad \varepsilon_t \sim \mathcal{N}(\boldsymbol{0}, \boldsymbol{I}) \tag{18}$$

where $\vec{\boldsymbol{F}}_t$, $\boldsymbol{\alpha}$, and β are all m dimensional column vectors, $\boldsymbol{\Sigma}$ is the covariance matrix, and $\boldsymbol{\varepsilon}_t$ is an $m-$dimensional standard normal random vector. $\boldsymbol{\alpha}$ now represents the optimal spatial filter, and $\boldsymbol{\beta}$ represents the baseline for each pixel. Our goal then is to estimate $\boldsymbol{\alpha}$ and $\boldsymbol{\beta}$, to provide maximal information about the underlying spike train. We would expect this optimal spatial filtering improve the effective SNR after filtering in many situations. For example, if certain pixels are anti-correlated with others, a uniform spatial filter would average out those differences, whereas the optimal filter would take advantage of that information.

To estimate $\boldsymbol{\alpha}$ and $\boldsymbol{\beta}$, we first plug Eqs (18) and (2) into (9), to obtain:

$$\vec{\boldsymbol{\theta}} = \underset{\vec{\boldsymbol{\theta}} \in \vec{\boldsymbol{\Theta}}}{\operatorname{argmax}} -\frac{T}{2}\log(2\pi|\boldsymbol{\Sigma}|) + T\log(\lambda\Delta) - \lambda\Delta\boldsymbol{n}'\boldsymbol{1}$$

$$-\frac{1}{2}\sum_{t=1}^{T}(\vec{\boldsymbol{F}}_t - \boldsymbol{\alpha}(\gamma\widehat{C}_{t-1} - \nu - \rho\widehat{n}_t) - \boldsymbol{\beta})'\boldsymbol{\Sigma}^{-1}(\vec{\boldsymbol{F}}_t - \boldsymbol{\alpha}(\gamma\widehat{C}_{t-1} - \nu - \rho\widehat{n}_t) - \boldsymbol{\beta}) \tag{19}$$

where $|\cdot|$ indicates the determinant. By pre-whitening the observation matrix, $\vec{\boldsymbol{F}} = [\vec{\boldsymbol{F}}_1, \vec{\boldsymbol{F}}_2, \ldots, \vec{\boldsymbol{F}}_T]$, we can estimate the covariance matrix by the identity, i.e., $\boldsymbol{\Sigma} = \boldsymbol{I}$. Without loss of generality, we may assume that $\nu = 0$ and $\rho = 1$, similar to our assumption of $\boldsymbol{\alpha} = 1$ and $\beta = 0$ above. This leaves γ, $\boldsymbol{\alpha}$, and $\boldsymbol{\beta}$. Assuming that γ is known (or estimated from the raw fluorescence signal, as we did above), we have:

$$\widehat{\boldsymbol{\eta}}_v = \underset{\|\boldsymbol{\eta}_v\|<1}{\operatorname{argmax}} \left\|\vec{\boldsymbol{F}} - \boldsymbol{\eta}_v \boldsymbol{X}_v\right\|^2 \tag{20}$$

where $\boldsymbol{\eta}_v = [\boldsymbol{\alpha}, \boldsymbol{\beta}]$, and $\boldsymbol{X}_v = [\gamma\boldsymbol{C} + \boldsymbol{n}, \boldsymbol{1}]'$. Note that we have constrained the norm of $\boldsymbol{\eta}_v$, which is necessary because otherwise there is a free scale between $\boldsymbol{X}_v$ and $\boldsymbol{\eta}_v$. Problems of the form as in Eq (20) are known as "trust region subproblems". Fortunately, many algorithms for solving such a problem are available [Fortin, 2000].
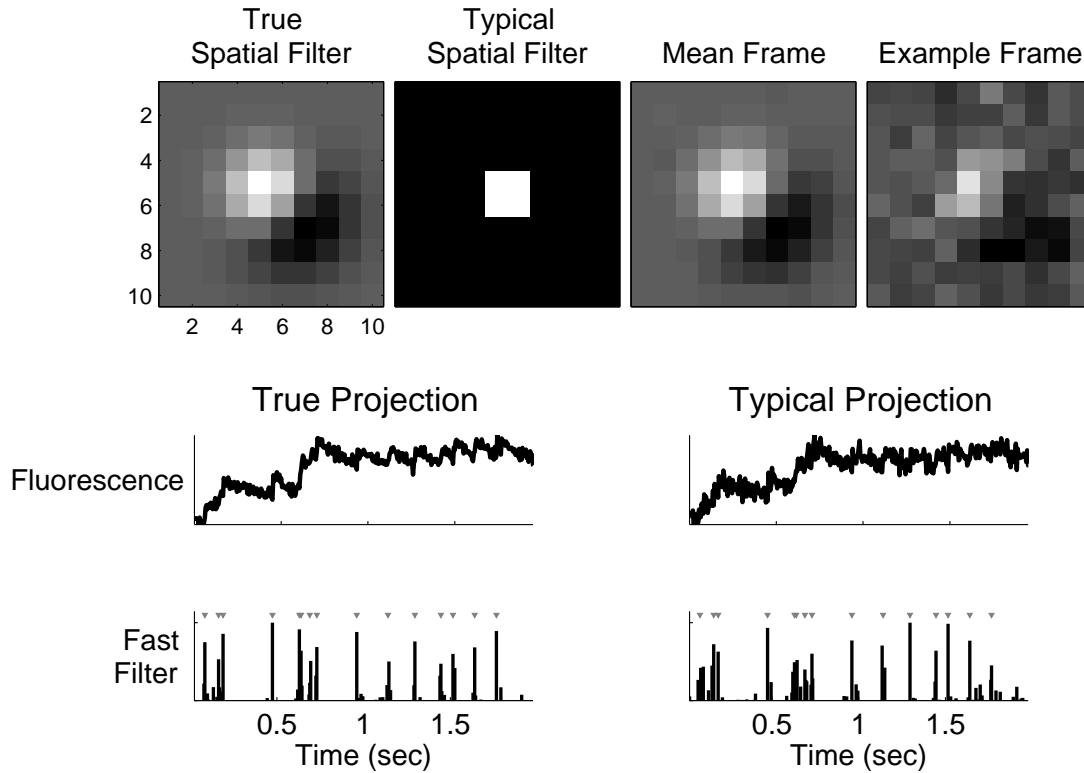
Figure 3: A simulation demonstrating that using a better spatial filter can significantly enhance the effective SNR (see Supplementary Movie 1 for the full movie associated with this simulation). Top: four movie frames. Middle left: projection of the entire movie onto the optimal spatial filter, yielding a 1D fluorescence time series, with a large SNR. Bottom left: fast filter's inferred spike train using the optimal spatial filter. Middle right: projection of the entire movie onto the "mean" spatial filter, yielding a 1D fluorescence time series with a small SNR. Bottom right: fast filter's inferred spike train using the mean spatial filter. Parameters different from Fig 1: α is a mixture of two 2D-Gaussians, with mean $\mu_1 = \mu_2 = [0, 0]$ and covariance matrices, $\Sigma_i = \sigma_i^2 I$, with $\sigma_1 = 2$ and $\sigma_2 = 4$ and I is the identity matrix. $\beta = 1$.
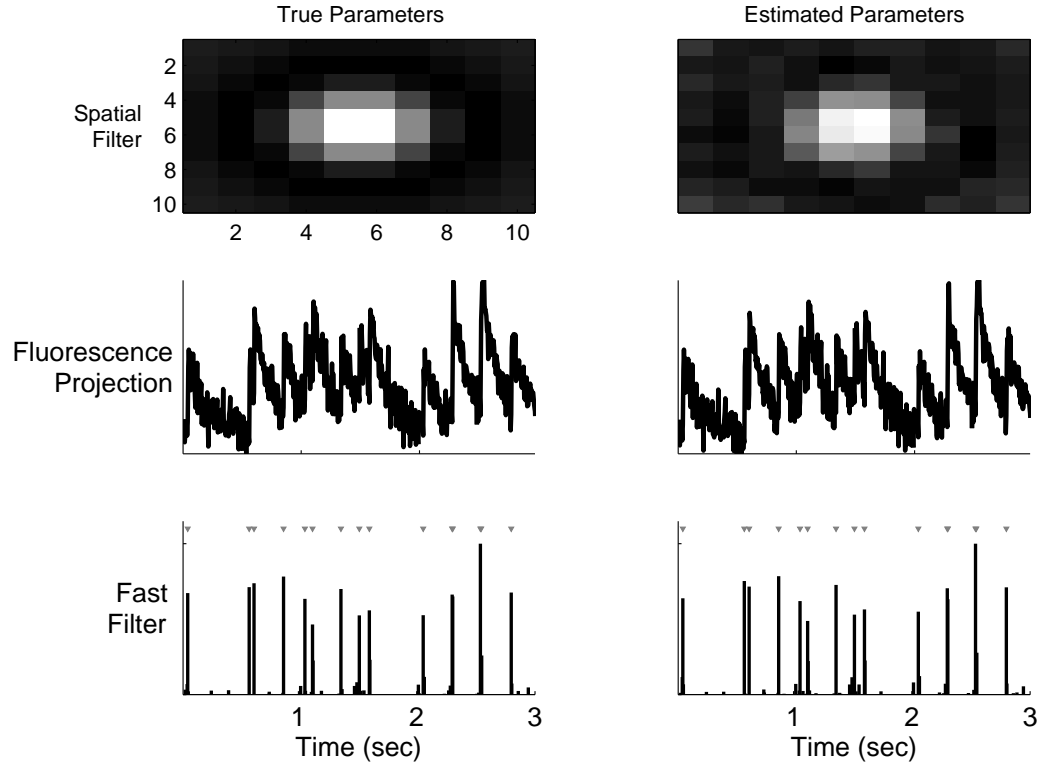
Figure 4: A simulation demonstrating that given only the fluorescence movie, the parameters may be estimated, and the spike train inferred (c.f. Supplementary Movie 2). Top left panel: true spatial filter. Middle left panel: projection of movie onto true spatial filter. Bottom left panel: inferred spike train using true parameters. Right panels: same as left except estimating parameters. α initialized with the first singular value of F. β initialized with 0. λ and σ were initialized at double their true value. τ was assumed known. Parameters same as above.

3.4   in vivo data

Mean Movie Frame

Spatial Filter
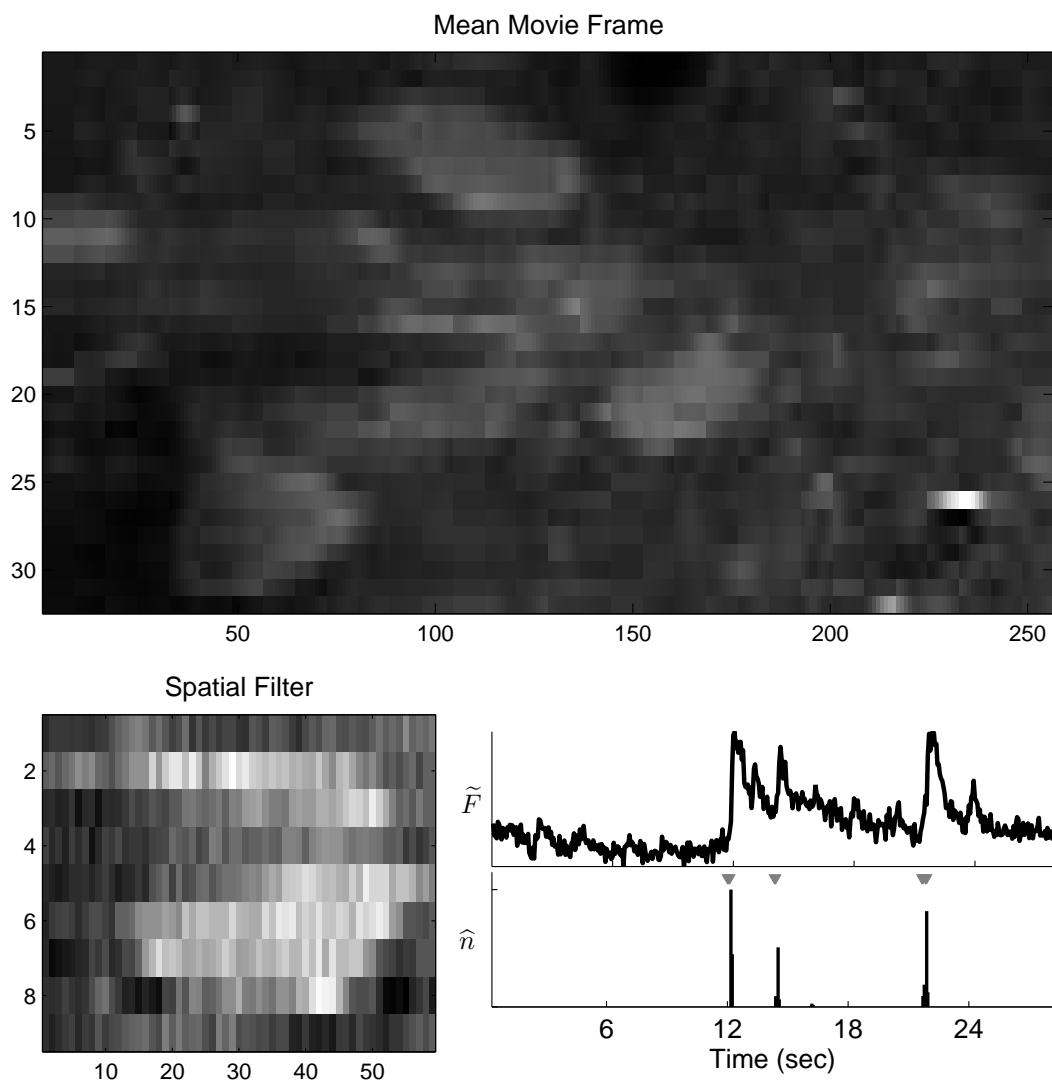
$\widetilde{F}$

$\widehat{n}$

Time (sec)

Figure 5: Given only a fluorescence movie, recorded in vivo, we can learn the parameters necessary to correctly infer the spike trains. Left: mean frame. Left: projection of movie onto mean frame. Left: the fast filter's inference.

Figure 6: distribution of errors in spike inference from real data
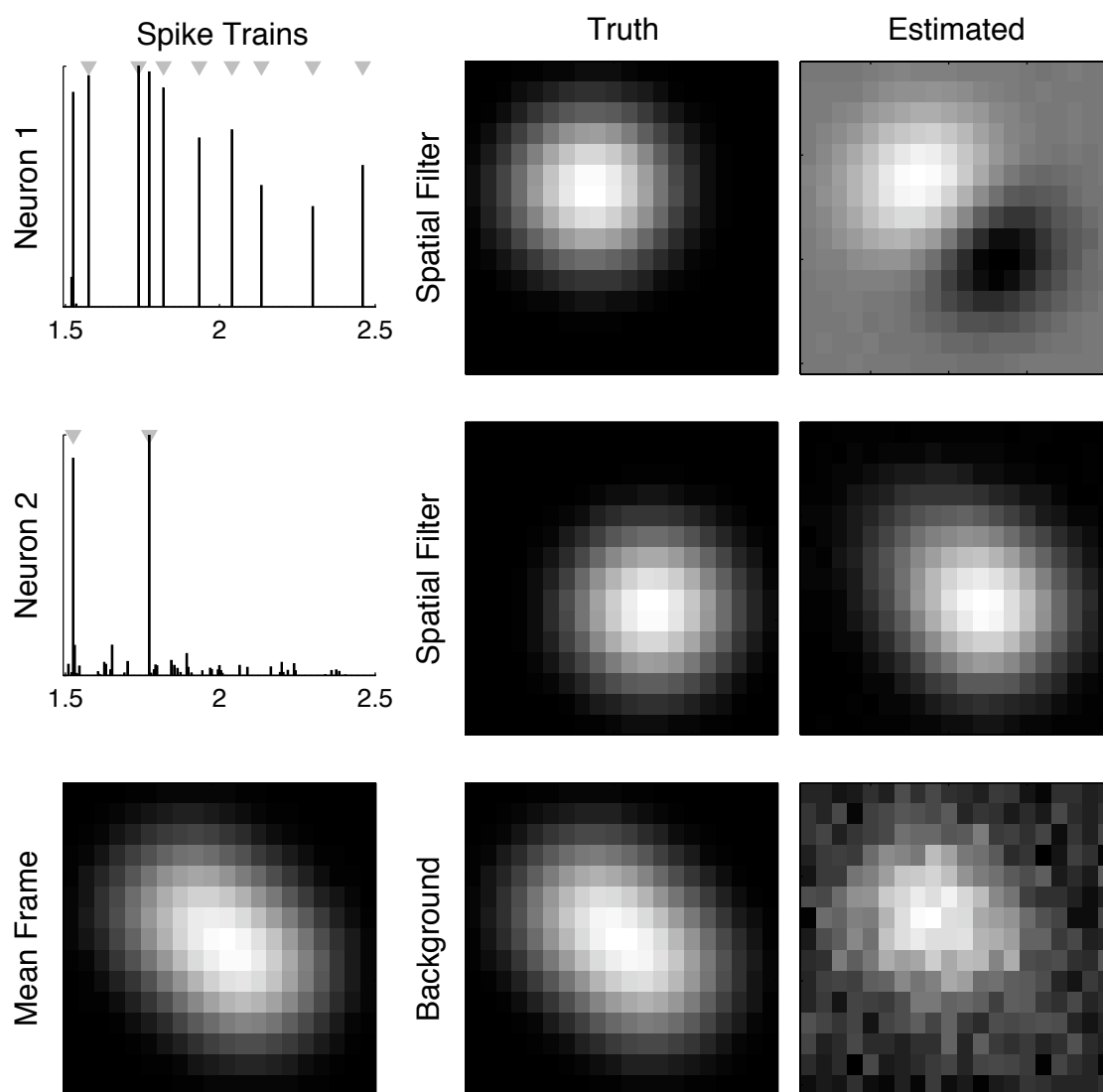
3.5 Overlapping spatial filters

Figure 7: Simulation showing that even when two neuron's spatial filters are largely overlapping, our inferencsame as spatial EM, but with 2 cells in ROI

3.6   Analyzing a whole movie

Figure 8: full movie, fully automated

Figure 9: full movie, fully automated, real data

3.7   Poisson observation model

3.8   Time varying prior

3.9   Slow dynamics

3.10   Incorporating a nonlinear observation model

3.11   Optimal thresholding

4 Discussion

We show here that for certain nonnegative deconvolution problems, we can derive an algorithm that is both optimal and efficient. More specifically, our algorithm may be applied to any model with a nonnegative signal that is linearly filtered by a matrix linear ordinary differential equation. We apply this approach to the problem of inferring the most likely spike train given noisy calcium sensitive fluorescence observations (c.f. Fig. **??**), and demonstrate, in simulations, that the optimal nonnegative filter outperforms the optimal linear (i.e., Wiener) filter in both slow and fast firing rate regimes (c.f. Fig. **??**). Furthermore, when applied to data from a live cell, the optimal nonnegative filter outperforms a fast projection pursuit regression filter, which constrains the inferred spike train to be nonnegative integers (c.f. Fig. **??**). On the other hand, the nonnegative filter is based on a linear observation model, and therefore suffers a loss of precision in the presence of strong saturation effects, in contrast to the optimal nonlinear particle filter (c.f. Fig. **??**).

The implications of these results are severalfold. First, it seems as if there is no reason to use the Wiener filter for scenarios in which our algorithm may apply. Second, as our filter is so efficient, it may be used for many real-time processing applications. Specifically, upon simultaneously imaging a population of neurons [Ikegaya et al., 2004, Niell and Smith, 2005, Ohki et al., 2005, Yaksi and Friedrich, 2006, Sato et al., 2007], our filter may be applied essentially online. This could greatly expedite the tuning of important experimental parameters — such as laser intensity — to optimize signal-to-noise ratio for inferring spikes. Third, the parameters estimated from this filter may be used to initialize the parameters of the optimal nonlinear particle filter, which may then be used offline, to further refine the spike train inference.

References

[Boyd and Vandenberghe, 2004] Boyd, S. and Vandenberghe, L. (2004). *Convex Optimization*. Oxford University Press.

[Fortin, 2000] Fortin, C. (2000). *A Survey of the Trust Region Subproblem within a Semidefinite Framework*. PhD thesis, University of Waterloo.

[Hastie et al., 2001] Hastie, T., Tibshirani, R., and Friedman, J. (2001). *The Elements of Statistical Learning: Data Mining, Inference, and Prediction*. Springer.

[Ikegaya et al., 2004] Ikegaya, Y., Aaron, G., Cossart, R., Aronov, D., Lampl, I., Ferster, D., and Yuste, R. (2004). Synfire chains and cortical songs: temporal modules of cortical activity. *Science*, 304(5670):559–564.

[Niell and Smith, 2005] Niell, C. M. and Smith, S. J. (2005). Functional imaging reveals rapid development of visual response properties in the zebrafish tectum. *Neuron*, 45(6):941–951.

[Ohki et al., 2005] Ohki, K., Chung, S., Ch'ng, Y. H., Kara, P., and Reid, R. C. (2005). Functional imaging with cellular resolution reveals precise micro-architecture in visual cortex. *Nature*, 433(7026):597–603.

[Rabiner, 1989] Rabiner, L. R. (1989). A Tutorial on Hidden Markov Models and Selected Applications in Speech Recognition. *Proceedings of the IEEE*, 72(2):257–286.

[Sato et al., 2007] Sato, T. R., Gray, N. W., Mainen, Z. F., and Svoboda, K. (2007). The functional microarchitecture of the mouse barrel cortex. *PLoS Biol*, 5(7):e189.

[Shumway and Stoffer, 2006] Shumway, R. and Stoffer, D. (2006). *Time Series Analysis and Its Applications*. Springer, 2nd edition.

[Wiener, 1949] Wiener, N. (1949). *Extrapolation, interpolation, and smoothing of stationary time series: with engineering applications*. MIT Press, Cambridge, Mass.

[Yaksi and Friedrich, 2006] Yaksi, E. and Friedrich, R. W. (2006). Reconstruction of firing rate changes across neuronal populations by temporally deconvolved Ca^{2+} imaging. *Nat Methods*, 3(5):377–383.

A   Wiener Filter

Sections 2.2 and 2.3 outline one approach to solving Eq. (3), by approximating the Poisson distribution with an exponential distribution, and imposing a non-negative constraint on the inferred $\widehat{n}$. Perhaps a more straightforward approach would be to approximate the Poission distribution with a Gaussian distribution. In fact, as rate increases above about 10 spikes/sec, a Poisson distribution with rate $\lambda\Delta$ is well approximated by a Gaussian with mean and variance $\lambda\Delta$. Given such an approximation, instead of Eq. (4), we would obtain:

$$\widehat{\boldsymbol{n}}_w \approx \operatorname*{argmin}_{n_t \in \mathbb{R}, \forall t} \sum_{t=1}^{T} \left(\frac{1}{2\sigma^2}(F_t - C_t)^2 + \frac{1}{2\lambda\Delta}(n_t - \lambda\Delta)^2 \right) \tag{21}$$

As above, we can rewrite Eq. (21) in matrix notation in terms of $\boldsymbol{C}$:

$$\widehat{\boldsymbol{C}}_w = \operatorname*{argmin}_{C_t \in \mathbb{R}, \forall t} \frac{1}{2\sigma^2} \|\boldsymbol{F} - \boldsymbol{C}\|^2 + \frac{1}{2\lambda\Delta} \|\boldsymbol{MC} - \lambda\Delta\boldsymbol{1}\|^2 \tag{22}$$

which is quadratic in $\boldsymbol{C}$, and may therefore be solved analytically using quadratic programming, $\widehat{\boldsymbol{C}}_w = \widehat{\boldsymbol{C}}_0 + \boldsymbol{d}_w$, where $\widehat{\boldsymbol{C}}_0$ is the initial guess and $\boldsymbol{d}_w = \boldsymbol{H}_w \backslash \boldsymbol{g}_w$, where

$$\boldsymbol{g}_w = \frac{1}{\sigma^2}(\boldsymbol{C}_0' - \boldsymbol{F}) + \frac{1}{\lambda\Delta}((\boldsymbol{M}\widehat{\boldsymbol{C}}_0)'\boldsymbol{M} - \lambda\Delta\boldsymbol{M}'\boldsymbol{1}) \tag{23}$$

$$\boldsymbol{H}_w = \frac{1}{\sigma^2}\boldsymbol{I} + \frac{1}{\lambda\Delta}\boldsymbol{M}'\boldsymbol{M} \tag{24}$$

Note that this solution is the optimal linear solution, under the assumption that spikes follow a Gaussian distribution, and if often referred to as the Wiener filter, regression with a smoothing prior, or ridge regression. To estimate the parameters for the Wiener filter, we take the same approach as above:

$$\widehat{\boldsymbol{\theta}}_w \approx \operatorname*{argmax}_{\boldsymbol{\theta}_w} P[\boldsymbol{F}|\widehat{\boldsymbol{n}}_w, \boldsymbol{\theta}_w]P[\widehat{\boldsymbol{n}}_w|\boldsymbol{\theta}_w] \tag{25a}$$

$$= \operatorname*{argmax}_{\boldsymbol{\theta}_w} -\frac{T}{2}\log(4\pi^2\sigma^2\lambda\Delta) - \frac{1}{2\sigma^2}\|\boldsymbol{Y}_w + \boldsymbol{\eta}_w\boldsymbol{X}_w\|^2 - \frac{1}{2\lambda\Delta}\|\widehat{\boldsymbol{n}}_w - \lambda\Delta\boldsymbol{1}\|^2 \tag{25b}$$

where $\boldsymbol{Y}_w$, $\boldsymbol{\eta}_w$, and $\boldsymbol{X}_w$ are defined as their subscriptless counterparts in Eq. (9).